

Influence of current density on oxygen transfer in an electroflotation cell

L. Ben Mansour · K. Kolsi · I. Ksentini

Received: 27 October 2006 / Revised: 20 March 2007 / Accepted: 21 March 2007 / Published online: 20 April 2007
© Springer Science+Business Media B.V. 2007

Abstract The objective of this work is to study the transfer of oxygen from gas to liquid phase in an electroflotation cell. The measurements were performed in a laboratory scale cell using insoluble electrodes, titanium coated with ruthenium oxide as anode and stainless steel as cathode. The volumetric mass transfer coefficient $K_L a$, was characterized for clean tap water as liquid phase for different values of current density (J). The global coefficient of mass transfer based on the liquid film, K_L , and the specific interfacial area, a , were characterized. A model which relates $K_L a$ to current density was established. Different evaluation criteria of oxygen transfer in electroflotation process were determined and compared with other aeration process.

Keywords Current density · Electroflotation · Oxygen transfer

Nomenclature

a	specific interfacial area ($\text{m}^2 \text{m}^{-3}$)
A	gas-liquid interface area (m^2)
C	oxygen concentration in the liquid (g m^{-3})
C^*	oxygen equilibrium concentration in the liquid (g m^{-3})
C_0	initial dissolved oxygen concentration (g m^{-3})
J	current density (A m^{-2})
d_B	bubble diameter (μm)
F	Faraday constant (C mol^{-1})
H_S	static height of the liquid bed (m)
H_T	total height of the gas – liquid bed (m)
K_L	global coefficient of mass transfer based on liquid film (m s^{-1})

$K_L a$	volumetric mass transfer coefficient (s^{-1})
m_{O_2}	oxygen flow rate (g s^{-1})
M_{O_2}	oxygen molar mass (g mol^{-1})
OC	oxygenation capacity ($\text{g m}^{-3} \text{h}^{-1}$)
RO	oxygenation efficiency (%)
S	surface of the electrodes (m^2)
T	temperature of the liquid phase ($^\circ\text{C}$)
V	aerated liquid volume (m^3)

Greek symbols

ε_g	gas hold-up (%)
θ	empirical coefficient in Eq. (7)

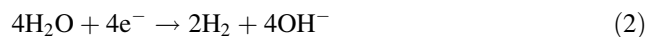
1 Introduction

Electroflotation (EF) was first proposed by Elmore in 1904 for flotation of valuable minerals from ores [1]. EF is a process that floats pollutants to the surface of a water body by small bubbles of hydrogen and oxygen generated by water electrolysis [2]. The electrochemical reactions at the cathode and the anode are hydrogen evolution and oxygen evolution, respectively.

Anodic oxidation



Cathodic reduction



Chen [3] has shown that EF is more competitive than other flotation technologies such as dissolved air flotation and dispersed air flotation.

L. B. Mansour (✉) · K. Kolsi · I. Ksentini
Sciences Faculty of Sfax, Laboratory of Water – Environment
and Energy, B.P. 802, Sfax 3018, Tunisia
e-mail: lassaadbenmansour@yahoo.fr

The effectiveness of the process is limited not only to the elimination of the polluting substances but also to the abatement of the dissolved organic matter by oxygen generated at the anode. Most available electroflotation process data has shown the effect of EF process in decreasing Chemical Oxygen Demand (COD) but without detailing the transfer phenomena [4–7].

The purpose of the present work is to study oxygen transfer in tap water during electroflotation. In order to achieve this objective, the volumetric mass transfer coefficient, $K_L a$, at different current densities J must be evaluated. $K_L a$ is the parameter which characterizes the gas-liquid mass transfer and is one of the most important parameters in the design and scale-up of aeration systems. Several authors have dissociated $K_L a$ into the volumetric interfacial area, a , and the global coefficient of mass transfer based on the liquid film, K_L , [8, 9]. These two parameters have been determined in this study.

A comparative study with other aeration systems has been made and a model is also proposed based on the relationship between, $K_L a$, and current density J .

2 Theory

To determine the volumetric mass transfer coefficient, $K_L a$, several techniques have been proposed. Most measurements in aeration systems may be divided into two groups: physical and chemical methods [10]. Among physical methods, the well-known method is the desorption of an oxygen saturated solution with nitrogen [11, 12]. Many chemical methods such as oxidation of glucose [13], stannous chloride [14], and ethanol [15] have been proposed. In the present work we have adapted the sulphite oxidation method which is the most widespread technique for determining the volumetric oxygen transfer coefficient and the interfacial area per unit of volume [16–18].

For clean tap water the double Film Theory of Lewis and Whitman is considered [19]. For gases of low solubility, such as oxygen in water, Lewis and Whitman assumed that the gas side resistance is negligible and that the gas transfer may be determined from considering the liquid side resistance only:

$$\frac{dC}{dt} = K_L \frac{A}{V} (C^* - C) \quad (3)$$

$$\frac{dC}{dt} = K_L a (C^* - C) \quad (4)$$

Equation (4) can be readily integrated to yield the following expression for C as a function of time

$$C = C^* - (C^* - C_0) \exp(-K_L a t) \quad (5)$$

where C_0 is the initial dissolved oxygen concentration at $t = 0$. A nonlinear regression analysis based on the Gauss–Newton method is recommended by ASCE to fit eq. (5) to experimental data using $K_L a$, C^* and C_0 as three adjustable model parameters [20].

3 Materials and methods

3.1 Materials

3.1.1 Electroflotation cell

The electroflotation cell, shown in Fig. 1, was a rectangular column. Its length was 5.8 cm, its width 6.7 cm and its height 71.5 cm. It was provided with two electrodes: titanium coated with ruthenium oxide anode and a stainless steel cathode. These two electrodes were supplied by a D.C. power supply. The electrodes were placed on the bottom of the cell. An electrode arrangement proposed and tested by Chen et al. was used, [21] which allows the inter-electrode gap to be as small as 2 mm (Fig. 2).

3.2 Methods

3.2.1 Volumetric mass transfer coefficient

The volumetric mass transfer coefficient, $K_L a$, was measured using the unsteady state method with an oxygen probe (DO meter WTW DurOx 325) placed mid-way in the electroflotation cell. The oxygen concentration was reduced to zero by adding 150 mg l⁻¹ of sodium sulphite (Na₂SO₃) and 2 mg l⁻¹ of cobalt ions.

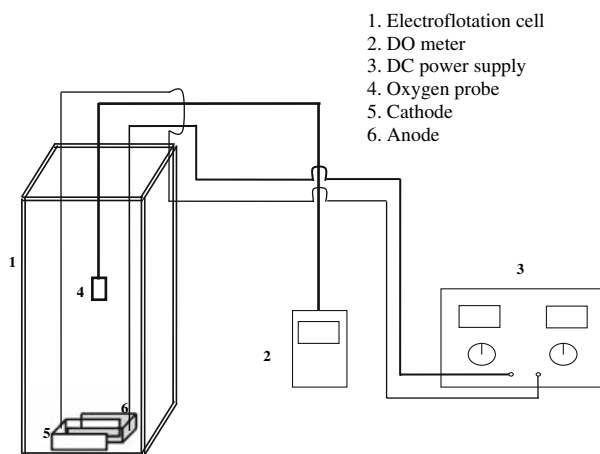


Fig. 1 Schematic diagram of the experimental set-up

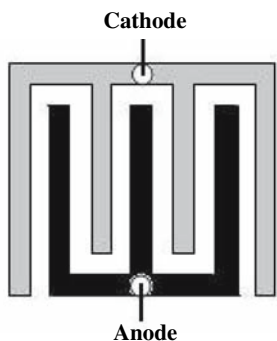


Fig. 2 Arrangement of electrodes

The response time of the oxygen probe is about 25 s. This duration does not affect the value of $K_L a$ determined under the experimental conditions.

The volumetric mass transfer coefficient was corrected to a standard reference temperature of 20 °C using the Arrhenius relationship with empirical coefficient $\theta = 1.0241$:

$$K_L a_{(20^\circ\text{C})} = K_L a_{(T)} \theta^{(20-T)} \tag{7}$$

3.2.2 Gas hold-up

Gas hold-up was determined by measuring the aerated liquid height relative to the gas-free liquid level using the bed height method [8]

Gas hold-up, ε_g , was calculated using Eq. (8):

$$\varepsilon_g = \frac{H_T - H_S}{H_T} \tag{8}$$

3.2.3 Bubble diameter

The bubble size was measured using the image analysis method. The equipment used was a microscopic zoom digital video camera (model NV-A3E from Panasonic, Japan), a magneto scope (model SVR-11G from Samsung Electronics), an acquisition card (model Pinnacle PCTV PRO version 4.02 from Pinnacle systems), a PC (model Pentium 4, from Fujitsu Siemens) with a digital image analysis program (model Photoshop version 7.0 from Adobe).

Most of the bubbles were ellipsoidal in shape and the local bubble diameter was calculated using the following relationship:

$$d_{Bi} = (x^2 y)^{\frac{1}{3}} \tag{9}$$

where x and y are the diameter and the width of the ellipsoid respectively. For a given current density, 150–200

bubbles were selected to estimate the Sauter mean diameter, d_B , calculated by Eq. (10):

$$d_B = \frac{\sum_{i=1}^n d_{Bi}^3}{\sum_{i=1}^n d_{Bi}^2} \tag{10}$$

where n is the number of bubbles with an individual diameter d_{Bi} .

4 Results and discussion

In order to calculate the volumetric mass-transfer coefficients from the ASCE model using eq. (5) a series of unsteady-state reoxygenation tests at different current densities were conducted. The results are shown in Fig. 3. All the data for different current densities show the same trend. The oxygen concentration increases at the beginning of the electrolysis process than stabilizes when it reaches the equilibrium concentration.

4.1 Volumetric mass transfer coefficient

The volumetric mass transfer coefficient, $K_L a$, is plotted as a function of current density in Fig. 4. $K_L a$, increases with current density up to 260 A m⁻² and then becomes almost constant. However, the volumetric mass transfer coefficient, $K_L a$, is the product of the global coefficient of mass transfer based on the liquid film, K_L , and the volumetric interfacial area, a . Consequently, these results can be explained by studying the variation of, a , and K_L with current density.

4.2 Gas hold-up

The gas hold-up, which is one of the most important parameters characterising the hydrodynamics of reactors,

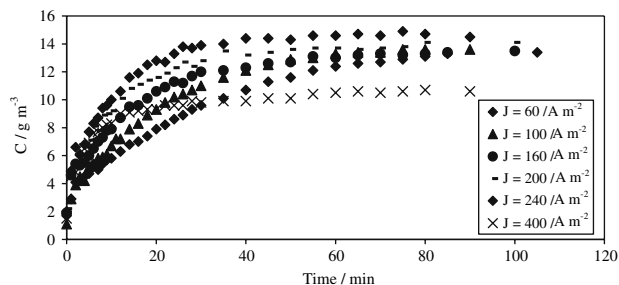


Fig. 3 Experimental unsteady-state reoxygenation curves at different current density

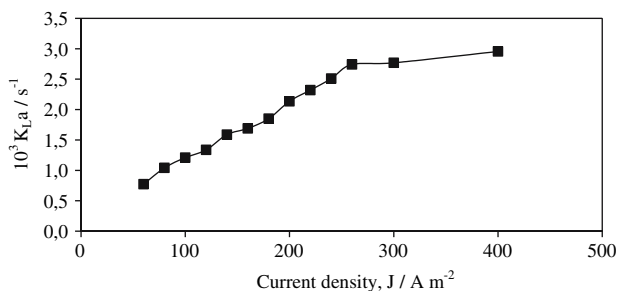


Fig. 4 Volumetric mass transfer coefficient versus current density

depends mainly on the gas velocity and physical properties of the liquid [22]. Figure 5 shows that ϵ_g increases with J . It has been also shown that the gas hold-up ϵ_g increases when the gas is efficiently dispersed and when gas velocity is increased [23, 24].

4.3 Bubble diameter

Figure 6 shows the effect of current density on bubble diameters, d_b increases almost linearly with J .

4.4 Volumetric interfacial area

The volumetric interfacial area is one of the most important parameters for gas–liquid reactor design. Generally, the interfacial area depends on the size of the unit, the operating parameters and the physical and chemical properties

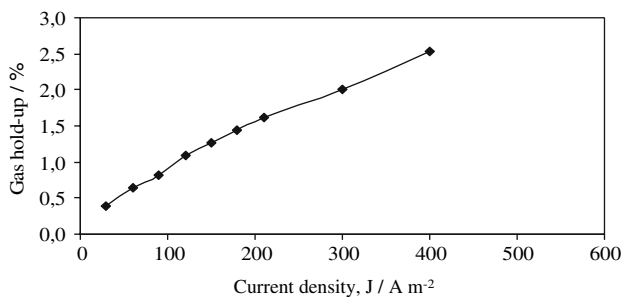


Fig. 5 Gas hold-up versus current density

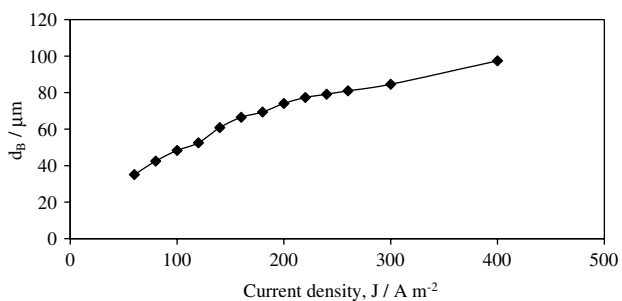


Fig. 6 Bubble diameter versus current density

of the liquid [25]. Knowing the bubble size and gas hold-up it is possible to evaluate the volumetric interfacial area:

$$a = \frac{6\epsilon_g}{d_B(1 - \epsilon_g)} \tag{11}$$

The variation of the volumetric interfacial area with current density is shown in Fig. 7.

The volumetric interfacial area ranges between 1101 and 1599 $m^2 m^{-3}$ for a current densities between 60 and 400 $A m^{-2}$. Figure 7 shows that, a , increases continuously with J . This can be explained by the absence of bubble coalescence even for high values of current density.

4.5 The global coefficient of mass transfer based on liquid film, K_L

The mass transfer rate depends not only on the gas hold-up and bubble size but also on the value of K_L . The global coefficient of mass transfer based on liquid film K_L depends on the diffusivity coefficient and turbulence created in the liquid phase. The K_L values were estimated by the following relationship:

$$K_L = K_L a \frac{d_B(1 - \epsilon_g)}{6\epsilon_g} \tag{12}$$

Figure 8 shows that K_L increases with increasing current density values up to 260 $A m^{-2}$ and then becomes almost constant at higher current densities.

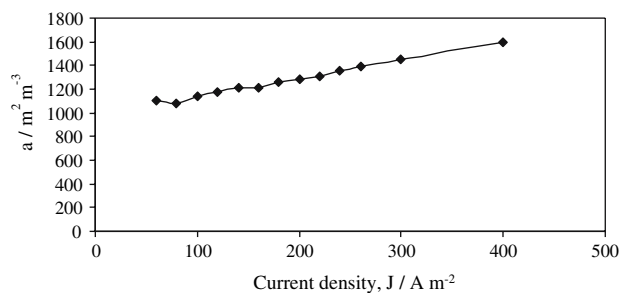


Fig. 7 Volumetric interfacial area versus current density

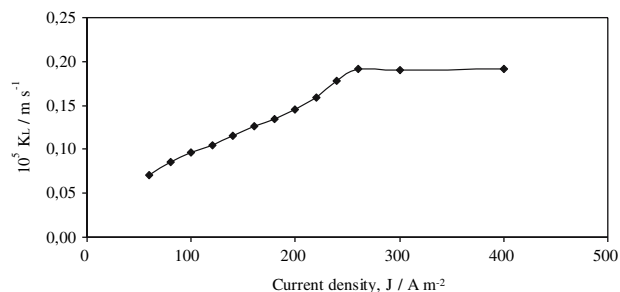


Fig. 8 Global coefficient of mass transfer based on liquid film versus current density

The results show that the K_L value increases with increasing current density. At higher current densities, a larger amount of oxygen was induced into the liquid phase, resulting in more gas bubbles. Consequently, turbulence created in the liquid phase was more intense. According to the two-film theory, the film thickness decreases with increasing turbulence due to the higher shear force. The mass transfer resistance therefore decreases and higher mass transfer rates can be obtained. Nevertheless, the value will reach a limiting value. This is similar to previous studies of other types of gas-inducing contactor [26, 27].

4.6 Relationship between $K_L a$ and J

The non-linear regression of the experimental data shown in Fig. 4 gives a model which relates the volumetric mass transfer coefficient with current density. The mathematical software used was DataFit (version 8.1.69).

Equation 13 shows the relationship between $K_L a$ and J .

$$K_L a = (1,796 \times 10^{-5}) J^{0.875} \tag{13}$$

Consequently, using Eq. (5), a relationship between the dissolved oxygen concentration and the current density can be established.

$$C = C^* - (C^* - C_0) e^{-((1.796 \times 10^{-5}) J^{0.875}) t} \tag{14}$$

As shown in Fig. 9 the obtained model fits the experimental data very well.

5 Comparison with other aeration systems

In order to evaluate the oxygen transfer rate using the electroflotation process, we have compared the results found with those of other oxygenation systems. The comparison is based on the oxygenation capacity (OC) and the oxygenation efficiency (RO).

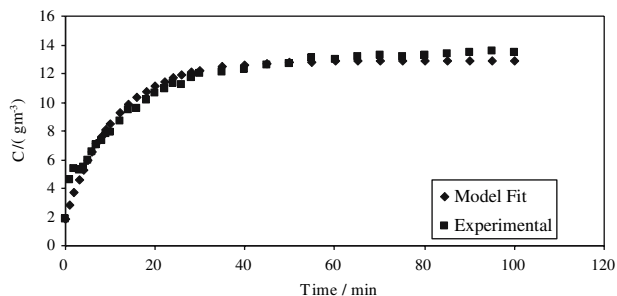


Fig. 9 Measured and calculated values of dissolved oxygen concentration for $J = 160 \text{ A m}^{-2}$

Table 1 Comparison between some aeration systems [28] and the present electroflotation process

Aeration systems	OC/ $\text{g m}^{-3} \text{ h}^{-1}$	RO/%
Diffusion		
Fine bubbles	120–200	20
Average bubbles	80–110	11
Large bubbles	80–110	9
Diffusion and Agitation		
Dorr-Oliver	60–80	8
Vortair	60–90	7
Mechanical aerator of surface		
Simplex	100–120	13
Brosse Kessener	120–200	14
Electroflotation	27–100	49–77

$$OC = K_L a (C^* - C_0) \tag{15}$$

$$RO = \frac{OC V}{m_{O_2}} 100 \tag{16}$$

m_{O_2} was determined by Faraday’s law:

$$m_{O_2} = \frac{JSM_{O_2}}{4F} \tag{17}$$

The results are given in Table 1.

The oxygenation capacity (OC) for the electroflotation is comparable to that of other aeration systems. The electroflotation process gives the highest oxygenation efficiency (RO). Indeed, for the majority of the systems (RO) does not exceed 21%, while for electroflotation (RO) can reach 77% which indicates the effectiveness of this process.

6 Conclusion

This work characterizes oxygen transfer in an electroflotation cell. The volumetric mass transfer coefficient, $K_L a$, was evaluated for clean tap water as liquid phase and for different values of current density, J . A model relating $K_L a$ to current density was established. The global coefficient of mass transfer based on the liquid film, K_L , and volumetric interfacial area, a , were dissociated. In order to compare electroflotation process to other aeration systems transfer criteria were calculated. The oxygenation efficiency (RO) of the electroflotation process is higher than that of other aeration systems and exceeds 75%.

References

1. Elmore FE (1905) Br Patent (13):578
2. Raju GB (1984) Trans Indian Inst Met 37(1):59
3. Chen G (2004) Sep Purif Technol 38:11

4. Mostefa NM, Tir M (2004) *Desalination* 161:115
5. Ge J, Qu J, Lei P, Liu H (2004) *Sep Purif Technol* 36:33
6. Murugananthan M, Raju GB, Prabhakar S (2004) *Sep Purif Technol* 40:69
7. Ben Mansour L, Ben Abdou Y, Gabsi S (2001) *Water Waste Environ Res* 2:51
8. Bouaifi M, Hebrard G, Bastoul D, Roustan M (2001) *Chem Eng Process* 40:97
9. Linek V, Moucha T, Kordac M (2005) *Chem Eng Process* 44:353
10. Deront M, Samb FM, Adler N, Péringer P (1998) *Chem Eng Sci* 53:1321
11. Reiss LP (1967) *I & EC Proc Des Dev* 6:486
12. Alexander BF, Shah YT (1976) *Can J Chem Eng* 54:556
13. Lee LL, Tsao GT (1972) *Chem Eng Sci* 27:1601
14. Filson GW, Walton JH (1932) *J Phys Chem* 36:740
15. Goto S, Mabuchi K (1984) *Can J Chem Eng* 62:865
16. Gchern JM, Chou SR, Shang CS (2001) *Wat Res* 35:3041
17. Linek V, Moucha T, Dousova M, Sinkule J (1994) *Biotechnol Bioeng* 43:477
18. Fujie K, Hu HY, Ikeda Y, Urano K (1992) *Chem Eng Sci* 47:3745
19. Lewis WK, Whitman WG (1924) *Ind Eng Chem* 16(12):1215
20. ASCE (1984) American Society of Civil Engineers
21. Chen X, Chen G, Yue PL (2002) *Environ Sci Technol* 36(4):778
22. Hébrard G, Bastoul D, Roustan M (1996) *Trans I Chem E* 74:406
23. Abrardi V, Rovero G, Sicardi S, Baldi G, Conti R (1990) *Trans Inst Chem Eng* 68:516
24. Chiampo F, Guglielmetti R, Manna R, Conti R (1991) Seventh European Conference on Mixing. Brugge, Belgium
25. Shah YT, Deckwer WD, Kelkar BG, Godbole SP (1982) *A I Ch E J* 28:353
26. Albal RS, Shah YT, Schumpe A (1983) *Chem Eng J Biochem Eng J* 27(2):61
27. Deimling A, Karandikar BM, Shah YT, Carr NL (1984) *Chem Eng J Biochem Eng J* 29(3):127
28. Edeline F (1984) *L'épuration physico-chimique des eaux théories et technologie* (4)